electronics

Article

Two Sound Field Control Methods Based on Particle Velocity

Song Wang and Cong Zhang *

School of Mathematics and Computer Science, Wuhan Polytechnic University, Wuhan 430048, China; wnsg2001@163.com
* Correspondence: hb_wh_zc@163.com

Abstract: In recent years, a variety of sound field control methods have been proposed for the generation of separated sound regions. Different algorithms control the physical properties of the generated sound field to different degrees. The existing methods mainly focus on sound pressure restoration and its related improvement. When the loudspeaker array is non-uniformly placed, the reconstruction system is not stable enough. To solve this problem, this paper proposes two sound field control methods related to particle velocity. The first method regulates the reconstruction error of particle velocity in the bright zone and the square of particle velocity in the dark zone; the second method regulates the reconstruction error of sound pressure and particle velocity in the bright zone and the square of sound pressure and particle velocity in the dark zone. Five channel and twenty-two channel non-uniform loudspeaker systems were used for two-dimensional and three-dimensional computer simulation testing. Experimental results show that the two proposed methods have better tradeoffs in terms of acoustic contrast, reproduction error and array effort than traditional methods, especially the second proposed method. In the two-dimensional experiment, the maximum reductions of the average array efforts generated by the proposed methods were about 10 dB and 11 dB compared with the average array efforts generated by two traditional methods. In the three-dimensional experiment, the maximum reductions of the average array efforts generated by the proposed methods were about 8 dB and 2 dB compared with the average array efforts generated by two traditional methods. The smaller the array effort, the more stable the loudspeaker system. Therefore, the reconstruction systems produced by the proposed methods are more stable than those produced by the traditional methods.

Keywords: sound field control; particle velocity; non-uniform loudspeaker systems

check for updates

Citation: Wang, S.; Zhang, C. Two Sound Field Control Methods Based on Particle Velocity. *Electronics* **2022**, *11*, 2275. https://doi.org/10.3390/electronics11142275

Academic Editor: Daniele Salvati

Received: 30 June 2022
Accepted: 18 July 2022
Published: 21 July 2022

1. Introduction

The existing sound field control methods based on loudspeaker array can be divided into two types: one method attempts to produce a sound field infinitely close to the desired sound field [1–21], including Ambisonics based on spherical harmonic decomposition and wave field synthesis (WFS) based on the Huygens's principle, and the other approach attempts to concentrate sound energy in one zone (the bright zone) and attenuate it in another zone (the dark zone) [22–27]. Though the first type of methods are beneficial for the reproduction of specific sound fields and can control the impinging wave front in the control zone [28], the source configurations of the first method are susceptible to greater limitations, particularly for WFS and Ambisonics [2,4]. The second type of method only considers sound energy and therefore cannot control wave front or the direction of sound wave propagation [29]. This paper focuses on the reconstruction of the desired sound field in one zone by using a loudspeaker array while weakening the reconstruction of the sound field in another zone.

Choi et al. have proposed a method to maximize the acoustic contrast between the bright zone and the dark zone, which is called the acoustic contrast control method (ACC) [22], but the ACC method is not designed to reduce the error between the desired sound field and the reconstructed sound field. Shin et al. proposed the energy difference maximization method (EMD) [26], which is closely related to the ACC method. The EMD method is used to optimize the energy difference between the bright zone and the dark zone, but the ACC method optimizes the energy ratio between the bright zone and the dark zone. Pressure matching (PM) is a numerical optimization method to make the reconstructed sound field approximate to the desired sound field [30], which could be seen as an extension of study [3]. Chang et al. proposed a combined acoustic contrast maximization and pressure matching method [29] by adjusting the weights factor to determine the sound energy in the dark zone and the sound field reconstruction error in the bright zone. With the change of the weight factor between 0 and 1, the solution of the combined acoustic contrast maximization and pressure matching method changes between the acoustic contrast control method and the pressure matching method. Bai et al. proposed two sound field synthesis methods for minimal external radiation [31], which keeps the sound pressure reconstruction error minimum inside the loudspeaker array (the bright zone) and radiation minimum outside the loudspeaker array (the dark zone). The first method is the pressure-constrained method, which constrains sound pressure in the dark zone and with the objective function to minimize the error of the reconstructed sound pressure in the bright zone; the second method is the pressure–velocity-constrained method, which constrains sound pressure and particle velocity in the dark zone with the objective function also to minimize the error of the reconstructed sound pressure in the bright zone. Based on the pressure matching method, Olivieri et al. proposed a beamforming method [32]. By selecting control points that depend on frequency and are located on a half ring, this method finds balance between reconstructed sound field quality at the bright point and directivity with a linear loudspeakers array. Later, using compact loudspeaker arrays, they proposed two methods based on the pressure matching method to accurately reconstruct the target sound signal: the weighted pressure matching method and the linearly constrained pressure matching method [33]. In the zone without accurately reproducing the target, the weight value of the reconstruction error is low with the weighted pressure matching method; the linearly constrained pressure matching method imposes linear constraints on the reconstruction accuracy of the target signal in the specified zone. Experimental results show that the weighted pressure matching method has a good balance between the accuracy and directional performance of sound field reconstruction. Additionally, in study [34], they proposed a private sound system based on a circular array and the weighted pressure matching method. The proposed system is suitable for different application scenarios. When the input energy is limited, users can control the quality and directivity tradeoff by setting the expected characteristics of the acoustic field frequency response in the listening zone. The weighted pressure matching method weight in the dark zone is set to control the tradeoff so that the input signal meets the expected constraints. Experimental results show that this method is effective over a wide range of frequencies. Badajoz et al. proposed a combined pressure matching and binaural control technique for distance and direction sensing [35], where a circular loudspeaker array is used to reconstruct the sound field of a nearby sound source. The pressure matching method is used to synthesize the incident acoustic field by minimizing the error between the desired and reconstructed sound fields, and the binaural control technique is used to reconstruct the interaural level differences (ILDs) and interaural time differences (ITDs). On the basis of the pressure matching method, Afghah et al. proposed replacing the traditional Tikhonov regularization method with the eigen decomposition pseudoinverse method to solve the loudspeaker distribution coefficient [36]. The proposed method is designed to optimize the dark point performance without affecting the bright point performance. Liao et al. proposed personal sound reproduction with the robust control method [37], which minimizes the acoustic energy in the dark zone while limiting the sound pressure error in the bright zone. The method is applied to local sound field reconstruction of vehicle sound system. Experimental results show that the performance of the proposed method is comparable to that of the algorithm proposed in [29]. Lee et al. proposed a framework named perceptual VAST [38], which takes into account the characteristics of the sound signal and human auditory perception to generate the perceptually optimized sound zone, but these characteristics are not taken into account by traditional methods. The listening test shows that the proposed method is superior to the ACC and PM methods in perception measurement: short-time objective intelligibility and perceptual evaluation of speech quality. Then, they have proposed using time-domain variable span trade-off filters or frequency-domain variable span trade-off filters to generate sound zone [39,40]. Minimization of weighted pressure error and energy method uses the weight factor to adjust the sound pressure error in the bright zone, sound energy in the dark zone and loudspeaker array effort [41]. To adjust the reconstructed sound field performance by the minimization of weighted pressure error and energy method linearly and in real time, Ryu et al. proposed a personal audio control method [42] in which the weights of loudspeaker arrays are simulated as simple continuous functions by using piecewise linear approximation (PLA). Experiments show that the proposed control method can achieve fine tuning and linear adjustment of reconstructed sound field performance, and the performance of the proposed control method is slightly reduced compared with that of the minimization of weighted pressure error and energy method. Additionally, there are some real-time sound control systems; Choi proposed two real-time sound control systems [43]. The first system uses 24 loudspeakers to fit into a flat-panel TV, which allows listeners at different locations to enjoy different sounds by suppressing interference between two sound zones. The second system allows listeners to control the sound source width and auditory scenery distance in real time, which consists of a linear loudspeaker array and touchpad interface.

The above research indicates that the research on the second type of sound field control method mainly focuses on the restoration of sound pressure within the bright zone and its related improvement techniques because the restoration of sound pressure could improve the accuracy of sound field reconstruction for listeners in the bright zone. However, when the loudspeaker array is non-uniformly placed, the reconstruction system is not stable enough, which is not conducive to practical application. In non-uniform loudspeaker layouts, the pressure matching method often requires too much source strength output, which is not conducive to sensing the position of the virtual source. When loudspeakers are distributed sparsely or irregularly, the pressure matching method has limitations due to spatial aliasing. However, the particle velocity matching method has no limit for the aliasing frequency because it controls the energy flow rather than the pressure on the control surface [44]. The study in reference [44] shows that when the loudspeaker array is non-uniformly placed, the control of particle velocity in a single region can obtain more stable loudspeaker strengths than the control of sound pressure in a single region. Some research suggests that sound can be described by sound pressure and particle velocity [45], so in the aspect of sound field control, particle velocity recovery is also of certain research significance. Therefore, two sound field control methods based on particle velocity are proposed in this paper. The first method regulates the reconstruction error of particle velocity in the range of the bright zone and the square of particle velocity in the range of the dark zone; the second method regulates the reconstruction error of sound pressure and particle velocity in the bright zone and the square of sound pressure and particle velocity in the dark zone. The advantages and disadvantages of the proposed methods and traditional methods in sound field control are evaluated by computer simulation.

The content of this paper is arranged as follows: Section 1 introduces the research process and the research content of this paper; Section 2 introduces two traditional sound field control methods, ACC and PM; Section 3 constructs two sound field control models based on sound particle velocity and finds their solutions; Section 4 introduces the comparison index of the different methods, the simulation results of the performance between proposed methods and traditional methods and analyzes and discusses the simulation results; and the last section gives the conclusion of this paper.

2. Traditional Sound Control Methods

2.1. Description of Sound Field in Dark Zone and Bright Zone

Figure 1 shows the placement structure of the loudspeaker array, and the locations of the bright zone and the dark zone. The center point of the coordinate system is origin O, multiple loudspeakers (suppose their number is M) are located on the same ring, and the bright zone and the dark zone are located inside the loudspeaker array. Suppose that there are m sample points $\vec{b}_1, \vec{b}_2, \cdots, \vec{b}_m$ in the bright zone, and n sample points $\vec{d}_1, \vec{d}_2, \cdots, \vec{d}_n$ in the dark zone. Then, the desired sound field at the sampling points within the range of the bright zone and the dark zone could be expressed as:

$$\begin{aligned} \overline{p_b} &= \left(p(\vec{b}_1), p(\vec{b}_2), \cdots, p(\vec{b}_m) \right)^T \\ \overline{p_d} &= \lambda \left(p(\vec{d}_1), p(\vec{d}_2), \cdots, p(\vec{d}_n) \right)^T \end{aligned} \tag{1}$$

where λ is amplitude control factor, which is used to regulate the amplitude of the dark zone. The energy in the dark region can be reduced by adjusting the value of λ. For example, the sound pressure amplitude in the dark zone could be attenuated by 60 dB. The sound field generated by the loudspeaker array at the sampling points in the range of the bright zone and the dark zone could be denoted as:

$$\begin{aligned} p_{lb} &= \sum_{j=1}^{M} G(\vec{ld}_j, \vec{b}) q_j \\ p_{ld} &= \sum_{j=1}^{M} G(\vec{ld}_j, \vec{d}) q_j \end{aligned} \tag{2}$$

where $G(\vec{ld}_j, \vec{b})$ represents sound pressure transfer function between loudspeaker at $\vec{ld}_j$ and any point $\vec{b}$ in the bright zone, $G(\vec{ld}_j, \vec{d})$ represents the sound pressure transfer function between loudspeaker at $\vec{ld}_j$ and any point $\vec{d}$ in the dark zone similarly. q_j represents loudspeaker strength. Equation (2) can be rewritten as follows:

$$\begin{aligned} \overline{p_{lb}} &= G_b q \\ \overline{p_{ld}} &= G_d q \end{aligned} \tag{3}$$

where:

$$q = (q_1, q_2, \cdots, q_M)^T \tag{4}$$

$$G_b = \begin{pmatrix} G(\vec{ld}_1, \vec{b}_1) & G(\vec{ld}_2, \vec{b}_1) & \cdots & G(\vec{ld}_M, \vec{b}_1) \\ G(\vec{ld}_1, \vec{b}_2) & G(\vec{ld}_2, \vec{b}_2) & \cdots & G(\vec{ld}_M, \vec{b}_2) \\ \cdots & \cdots & \cdots & \cdots \\ G(\vec{ld}_1, \vec{b}_m) & G(\vec{ld}_2, \vec{b}_m) & \cdots & G(\vec{ld}_M, \vec{b}_m) \end{pmatrix} \tag{5}$$

$$G_d = \begin{pmatrix} G(\vec{ld}_1, \vec{d}_1) & G(\vec{ld}_2, \vec{d}_1) & \cdots & G(\vec{ld}_M, \vec{d}_1) \\ G(\vec{ld}_1, \vec{d}_2) & G(\vec{ld}_2, \vec{d}_2) & \cdots & G(\vec{ld}_M, \vec{d}_2) \\ \cdots & \cdots & \cdots & \cdots \\ G(\vec{ld}_1, \vec{d}_n) & G(\vec{ld}_2, \vec{d}_n) & \cdots & G(\vec{ld}_M, \vec{d}_n) \end{pmatrix} \tag{6}$$

T is the transpose of the matrix and $\overline{p_{lb}}$ and $\overline{p_{ld}}$ are vectors.

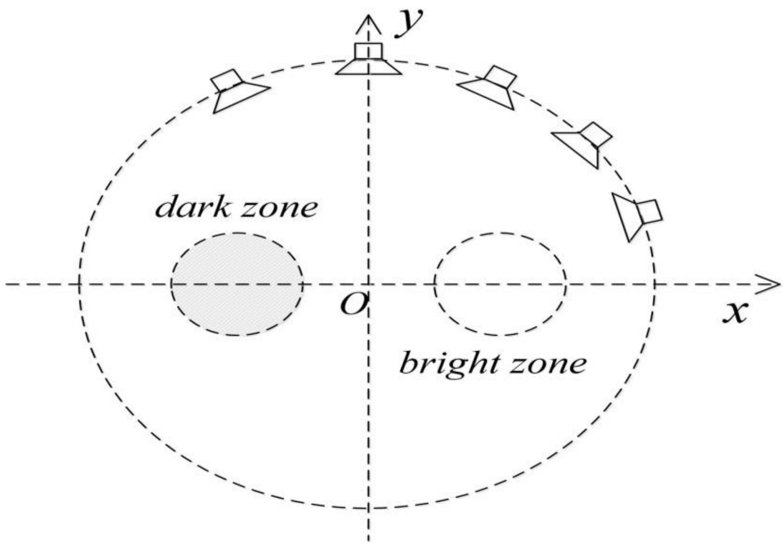

Figure 1. Loudspeaker array, bright zone and dark zone.

2.2. PM Method

The PM method attempts to reconstruct the sound field generated by the original sound source using a number of loudspeakers. To obtain the desired sound field in the bright zone, we could set up the equation as follows:

$$\overline{p_b} = G_b q \tag{7}$$

Then the solution of the PM method is:

$$q = G_b^+ \overline{p_b} \tag{8}$$

where + represents the pseudo inverse of a matrix. This is PM method in the bright zone. If we want to get the desired sound field both in the bright zone and the dark zone, we need another equation:

$$\overline{p_d} = G_d q \tag{9}$$

By combining Equations (7) and (9), we could obtain:

$$\overline{p} = \overline{G} q \tag{10}$$

where $\overline{p} = \left(\overline{p_b}^T \ \overline{p_d}^T\right)^T$, $\overline{G} = \left(G_b^T \ G_d^T\right)^T$. By solving Equation (10) and based on Tikhonov regularization, the loudspeaker strength of the PM method can be obtained as follows [36]:

$$q = \begin{cases} \left(\overline{G}^H \overline{G} + \beta I\right)^{-1} \overline{G}^H \overline{p}, & if(m+n) > M \\ \left(\overline{G} + \beta I\right)^{-1} \overline{p}, & if(m+n) = M \\ \overline{G}^H \left(\overline{G}\overline{G}^H + \beta I\right)^{-1} \overline{p}, & if(m+n) < M \end{cases} \tag{11}$$

where β is the regularization parameter, H is the Hermitian transpose, -1 is the inverse of a matrix and I is the identity matrix.

2.3. ACC Method

The ACC method is used to maximize the acoustic contrast between the bright zone and the dark zone [22]. Acoustic contrast is defined as the ratio of the sound potential energy density in the bright zone to the sound potential energy density in the dark zone. The greater the value of acoustic contrast, the greater the difference of sound pressure level between the bright zone and the dark zone [42]. The calculation formula of the sound potential energy density ζ in control zone Z is:

$$\begin{aligned} \zeta &= \frac{1}{Z_0}\int_Z p_z^H p_z dz \\ &= q^H\left(\frac{1}{Z_0}\int_Z G_z^H G_z dz\right)q \\ &= q^H W_z q \end{aligned} \tag{12}$$

where:

$$\begin{aligned} &p_z = G_z q \\ &G_z = \left(G(\vec{ld}_1, \vec{a}), G(\vec{ld}_2, \vec{a}), \cdots, G(\vec{ld}_M, \vec{a})\right) \end{aligned} \tag{13}$$

Z_0 is the volume of control zone, $\vec{a}$ is any point in control zone Z and W_z is the spatial correlation matrix. Similarly, the sound potential energy density ζ_b in the bright zone Z_b and the sound potential energy density ζ_d in the dark zone Z_d are, respectively:

$$\begin{aligned} \zeta_b &= q^H W_b q \\ \zeta_d &= q^H W_d q \end{aligned} \tag{14}$$

W_b and W_d are the spatial correlation matrix. The acoustic contrast is calculated by the following formula:

$$\eta_0 = \frac{\zeta_b}{\zeta_d} = \frac{q^H W_b q}{q^H W_d q} \tag{15}$$

The loudspeakers' optimal strength is the eigenvector corresponding to the maximum eigenvalue of matrix $W_d^{-1}W_b$ [25], which can maximize η_0. The mathematical expression is:

$$\left(W_d^{-1}W_b\right)q_{opt} = \eta_{max} q_{opt} \tag{16}$$

where q_{opt} is loudspeakers' optimal strength and η_{max} is the maximum eigenvalue.

2.4. The Advantages and Disadvantages of the PM Method and ACC Method

Each of the traditional methods described above has its own advantages and disadvantages. The PM method can reduce the error of reconstructed sound field in the bright zone, but it ignores acoustic contrast between the bright zone and the dark zone. The ACC method can increase the acoustic contrast between the bright zone and the dark zone, but it cannot reduce the error of the reconstructed sound field in the bright zone.

3. Proposed Methods

This section proposed two sound field control methods. The first method is based on particle velocity, and the second method is based on sound pressure and particle velocity. Suppose that $\vec{V}(\vec{ld}_j, \vec{b})$ is the particle velocity transfer function between loudspeaker at $\vec{ld}_j$ and any point $\vec{b}$ in the bright zone, $\vec{V}(\vec{ld}_j, \vec{d})$ represents particle velocity transfer function between loudspeaker at $\vec{ld}_j$ and any point $\vec{d}$ in the dark zone similarly. The particle velocity transfer function between loudspeaker at $\vec{ld}_j$ and point $\vec{b}$ is defined as [44]:

$$\vec{V}(\vec{ld}_j, \vec{b}) = \frac{ike^{-ikr}}{4\pi r}\left(1 + \frac{1}{ikr}\right)\frac{(\vec{b} - \vec{ld}_j)}{r} \tag{17}$$

where $r = |\vec{b} - \vec{ld}_j|$ is the distance between point $\vec{b}$ and $\vec{ld}_j$ and k is the wave number. The particle velocity at point $\vec{b}$ produced by the loudspeakers at $\vec{ld}_j$, $j = 1, 2, \cdots, M$, is defined as:

$$\vec{u}_{lb}(\vec{ld}_j, \vec{b}) = \sum_{j=1}^{M} \vec{V}(\vec{ld}_j, \vec{b})q_j \tag{18}$$

Similarly, the definition of the particle velocity transfer function and particle velocity between the loudspeaker at $\vec{ld}_j$ and point $\vec{d}$ can be obtained. So we can obtain the particle velocity at point $\vec{d}$ produced by the loudspeakers at $\vec{ld}_j$, $j = 1, 2, \cdots, M$:

$$\vec{u}_{ld}(\vec{ld}_j, \vec{d}) = \sum_{j=1}^{M} \vec{V}(\vec{ld}_j, \vec{d})q_j \tag{19}$$

Because particle velocity is a vector, it is not convenient to apply it directly in our model. We consider the concept of the radial particle velocity transfer function at point $\vec{b}$ and point $\vec{d}$:

$$\begin{aligned} V_r(\vec{ld}_j, \vec{b}) &= \vec{V}(\vec{ld}_j, \vec{b}) \cdot \vec{v}_r(\vec{b}) \\ V_r(\vec{ld}_j, \vec{d}) &= \vec{V}(\vec{ld}_j, \vec{d}) \cdot \vec{v}_r(\vec{d}) \end{aligned} \tag{20}$$

where $\vec{v}_r(\vec{b})$ and $\vec{v}_r(\vec{d})$ are the unite radial inward vector, which is normal to the surface of the bright zone and the dark zone, respectively. Then the radial particle velocity at point $\vec{b}$ and $\vec{d}$ produced by the loudspeakers at $\vec{ld}_j$, $j = 1, 2, \cdots, M$ can be obtained as follows:

$$\begin{aligned} u_{rlb}(\vec{ld}_j, \vec{b}) &= \sum_{j=1}^{M} V_r(\vec{ld}_j, \vec{b})q_j \\ u_{rld}(\vec{ld}_j, \vec{d}) &= \sum_{j=1}^{M} V_r(\vec{ld}_j, \vec{d})q_j \end{aligned} \tag{21}$$

Equation (21) can be written in matrix form:

$$\begin{aligned} \overline{u_{rlb}} &= V_{br}q \\ \overline{u_{rld}} &= V_{dr}q \end{aligned} \tag{22}$$

where $\overline{u_{rlb}}$ and $\overline{u_{rld}}$ are vectors,

$$V_{br} = \begin{pmatrix} V_r(\vec{ld}_1, \vec{b}_1) & V_r(\vec{ld}_2, \vec{b}_1) & \cdots & V_r(\vec{ld}_M, \vec{b}_1) \\ V_r(\vec{ld}_1, \vec{b}_2) & V_r(\vec{ld}_2, \vec{b}_2) & \cdots & V_r(\vec{ld}_M, \vec{b}_2) \\ \cdots & \cdots & \cdots & \cdots \\ V_r(\vec{ld}_1, \vec{b}_m) & V_r(\vec{ld}_2, \vec{b}_m) & \cdots & V_r(\vec{ld}_M, \vec{b}_m) \end{pmatrix} \tag{23}$$

$$V_{dr} = \begin{pmatrix} V_r(\vec{ld}_1, \vec{d}_1) & V_r(\vec{ld}_2, \vec{d}_1) & \cdots & V_r(\vec{ld}_M, \vec{d}_1) \\ V_r(\vec{ld}_1, \vec{d}_2) & V_r(\vec{ld}_2, \vec{d}_2) & \cdots & V_r(\vec{ld}_M, \vec{d}_2) \\ \cdots & \cdots & \cdots & \cdots \\ V_r(\vec{ld}_1, \vec{d}_n) & V_r(\vec{ld}_2, \vec{d}_n) & \cdots & V_r(\vec{ld}_M, \vec{d}_n) \end{pmatrix} \tag{24}$$

The cost function of the first proposed method is:

$$J_{V_r} = \mu \overline{u_{rld}}^H \overline{u_{rld}} + (1 - \mu)(\overline{u_{rlb}} - \overline{u_{rb}})^H (\overline{u_{rlb}} - \overline{u_{rb}}) \tag{25}$$

where $\overline{u_{rb}}$ and $\overline{u_{rd}}$ are the desired radial particle velocity at the sampling points within the range of the bright zone and the dark zone and are similar to the desired sound pressure in Equation (1). μ is the weighting factor and $0 < \mu < 1$, which adjusts the reconstruction error of radial particle velocity in the range of the bright zone and the square of radial particle velocity in the range of the dark zone. By combining Equations (22)–(25), we can obtain:

$$J_{V_r} = q^H \left(\mu V_{dr}^H V_{dr} + (1-\mu) V_{br}^H V_{br} \right) q + (1-\mu) \left(\overline{u_{rlb}}^H \overline{u_{rlb}} - \overline{u_{rlb}}^H V_{br} q - q^H V_{br}^H \overline{u_{rb}} \right) \quad (26)$$

Take the derivative of both sides of Equation (26) with respect to q, and set this formula equal to zero:

$$\frac{\partial J_{V_r}}{\partial q} = 2\left(\mu V_{dr}^H V_{dr} + (1-\mu) V_{br}^H V_{br} \right) q + 2(1-\mu) \left(-V_{br}^H \overline{u_{rb}} \right) = 0 \quad (27)$$

Then the global minimum of J_{V_r} can be obtained by Equation (27):

$$q_v = \left(\mu V_{dr}^H V_{dr} + (1-\mu) V_{br}^H V_{br} \right)^{-1} (1-\mu) V_{br}^H \overline{u_{rb}} \quad (28)$$

When $\mu = 0$, the optimal solution will minimize the reconstruction error of the radial particle velocity in the bright zone, and when $\mu = 1$, the optimal solution will minimize the square of the radial particle velocity in the dark zone. When μ is equal to some other value between 0 and 1, the optimal solution in Equation (28) varies between the case $\mu = 0$ and the case $\mu = 1$.

The cost function of the second proposed method is:

$$J_{PV_r} = \tau \overline{U_{ld}}^H \overline{U_{ld}} + (1-\tau)(\overline{U_{lb}} - \overline{U_b})^H (\overline{U_{lb}} - \overline{U_b}) \quad (29)$$

where:

$$\begin{aligned} \overline{U_{ld}} &= \left(\overline{p_{ld}}^T \overline{u_{rld}}^T \right)^T \\ \overline{U_{lb}} &= \left(\overline{p_{lb}}^T \overline{u_{rlb}}^T \right)^T \\ \overline{U_d} &= \left(\overline{p_d}^T \overline{u_{rd}}^T \right)^T \\ \overline{U_b} &= \left(\overline{p_b}^T \overline{u_{rb}}^T \right)^T \end{aligned} \quad (30)$$

τ is the weighting factor and $0 < \tau < 1$, which adjusts the reconstruction error of sound pressure and radial particle velocity in the range of the bright zone and the sound energy and square of radial particle velocity in the range of the dark zone. By combining Equations (3), (22), (29) and (30), we can obtain:

$$J_{PV_r} = q^H \left(\tau F_d^H F_d + (1-\tau) F_b^H F_b \right) q + (1-\tau)(\overline{U_{lb}}^H \overline{U_{lb}} - \overline{U_{lb}}^H F_b q - q^H F_b^H \overline{U_b}) \quad (31)$$

where:

$$\begin{aligned} F_d &= \left(G_d^T \; V_{dr}^T \right)^T \\ F_b &= \left(G_b^T \; V_{br}^T \right)^T \end{aligned} \quad (32)$$

Similar to the processing steps of Equation (27), we can obtain the optimal solution of J_{PV_r}:

$$q_{pv} = \left(\tau F_d^H F_d + (1-\tau) F_b^H F_b \right)^{-1} (1-\tau) F_b^H \overline{U_b} \quad (33)$$

When $\tau = 0$, the optimal solution will minimize the reconstruction error of the sound pressure and radial particle velocity in the bright zone, when $\tau = 1$, the optimal solution will minimize the sound energy and square of the radial particle velocity in the dark zone. When τ is equal to some other value between 0 and 1, the optimal solution in Equation (33) varies between the case $\tau = 0$ and the case $\tau = 1$. The convenience of the first and the second proposed method is that μ and τ can be set artificially. The second proposed method considers more physical properties (including sound pressure and radial particle velocity in the bright zone and the dark zone) than the first proposed method, which only considers radial particle velocity in the bright zone and the dark zone. The following simulation experiments compare and analyze the differences between them.

4. Simulations

In this part, the performance of the two proposed methods from Section 3 and the traditional methods from Second 2 in acoustic field control are compared through computer simulation experiments.

4.1. Indices of Sound Field Control

There are three performance indicators used to measure the sound field control effect of the different methods. The first performance indicator is acoustic contrast (AC), which is defined as described in detail in Section 2 and the calculation formula of which refers to formula (15). Acoustic contrast is used to measure the sound pressure level difference between the bright zone and the dark zone. We usually take the discrete [29] and logarithmic form of it, and its expression is as follows:

$$\eta = 10\log_{10}\left(\frac{\overline{p_{lb}}^H\overline{p_{lb}}/m}{\overline{p_{ld}}^H\overline{p_{ld}}/n}\right) \tag{34}$$

If a method results in a higher value of acoustic contrast, it means that this method works better [42]. The second performance index is reproduction error (RE), and its definition is the normalized spatial average error between the desired sound field and the reconstructed sound field in the bright zone, which is calculated by the following formula:

$$\epsilon = 10\log_{10}\left(\frac{(\overline{p_b} - \overline{p_{lb}})^H(\overline{p_b} - \overline{p_{lb}})}{\overline{p_b}^H\overline{p_b}}\right) \tag{35}$$

The normalized spatial average error is used to measure the reconstruction accuracy in the bright zone. If a method results in a lower value of normalized spatial average error in the bright zone, it means that this method works better [42]. The third performance index is array effort (AE), which is the sum of square of each loudspeaker's strength, with the following formula:

$$\kappa = 10\log_{10}\left(\sum_{j=1}^{M}|q_j|^2\right) \tag{36}$$

The array effort is used to measure the input of loudspeaker array and is closely related to the robustness of the playback system. If a method produces a lower value of array effort, it means that this method works better [42].

4.2. Experimental Setup

In practice, the loudspeaker array is often not evenly placed. So in the two-dimensional comparison experiment, the locations of the loudspeakers, the bright zone and the dark zone are shown in Figure 2. Five loudspeakers are placed non-uniformly on the same circle and make up a five-channel system. The distance between the center of the bright zone and the dark zone is 0.5 m, and the detailed locations of the loudspeakers, the bright zone, the dark zone and so on are shown in Table 1. In the three-dimensional comparison experiment, the locations of the loudspeakers, the bright zone and the dark zone are shown in Figure 3. Twenty-two loudspeakers are placed non-uniformly on the same sphere and make up a 22-channel system [46]. The distance between the center of the bright zone and the dark zone is 1.2 m, and the detailed locations of the loudspeakers, the bright zone, the dark zone and so on are shown in Table 2. For both the 5-channel system and 22-channel system, the bright zone and the dark zone are located inside the loudspeaker array. The bright zone and the dark zone have the same radius: 0.2 m, which can contain a listener's head. The whole coordinate system has the same origin. The speed of sound is 340 m/s. The function expression of the sound pressure transfer function is [33]:

$$G(\overrightarrow{ld}_j, \overrightarrow{a}) = \frac{e^{-ik|\overrightarrow{a} - \overrightarrow{ld}_j|}}{4\pi|\overrightarrow{a} - \overrightarrow{ld}_j|} \tag{37}$$

where $\overrightarrow{a}$ is any point in sound field. The frequency range of the original source signal is 100–1000 Hz. The interval between adjacent sampling points in the bright zone and the dark zone is approximately 0.036 m, which is less than one-ninth of the wavelength of the maximum frequency 1000 Hz. For convenience, such sampling points are denoted as dense sampling points. We set the weighting factors μ and τ equal to 0.1, 0.5 and 0.9, respectively.

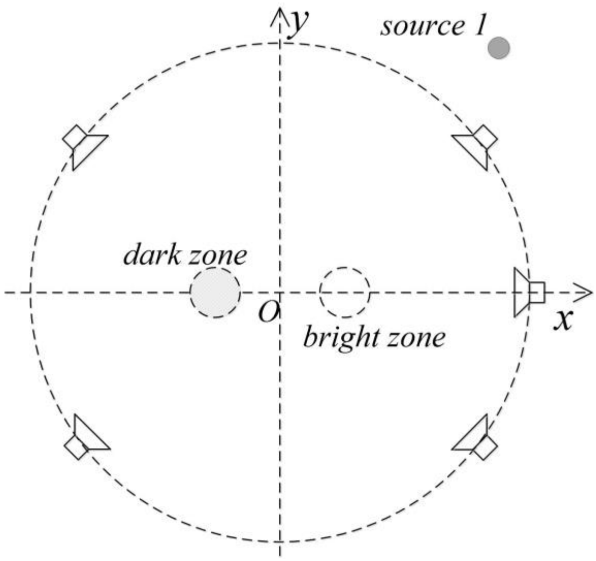

Figure 2. Diagram of 5-channel system setup.

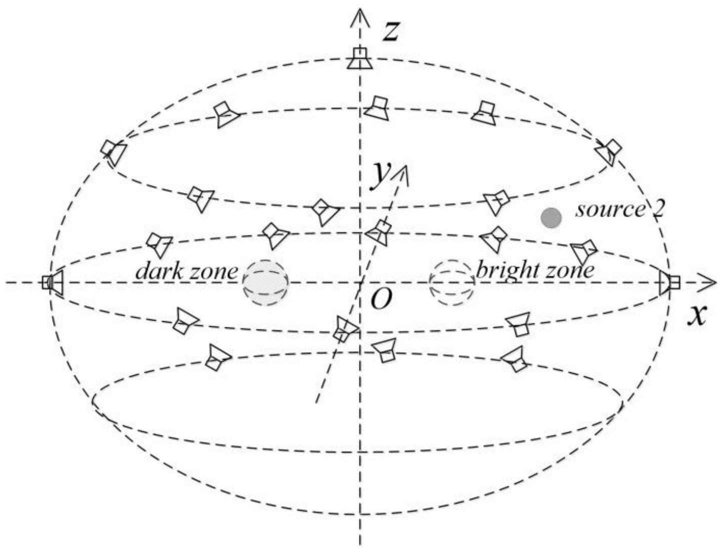

(**a**)

Figure 3. *Cont.*

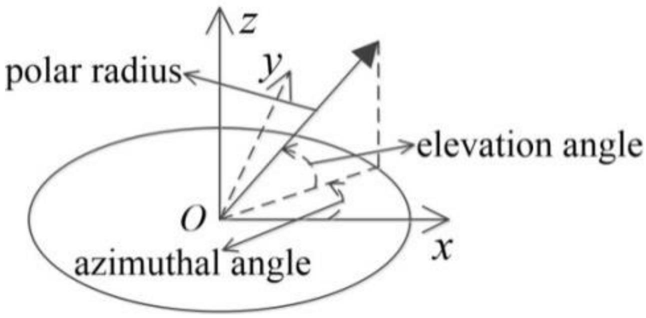

(**b**)

Figure 3. (**a**): Diagram of 22-channel system setup; (**b**): 3D coordinate system.

Table 1. The location of related points for experiment 1.

Point	Polar Radius	Azimuthal Angle
Center of dark zone	0.25 m	180°
Center of bright zone	0.25 m	0°
Loudspeaker 1	2 m	0°
Loudspeaker 2	2 m	45°
Loudspeaker 3	2 m	135°
Loudspeaker 4	2 m	225°
Loudspeaker 5	2 m	315°
Origin	0 m	0°
Original source 1	2.5 m	60°

4.3. Experimental Results

4.3.1. Two-Dimensional Experiment for 5-Channel System

Figure 4 shows the acoustic contrast comparison of different methods, including the PM method in the bright zone, the ACC method, the first proposed method and the second proposed method. The ACC method has the highest acoustic contrast, while the PM method in the bright zone has the lowest acoustic contrast for most frequencies. The reason is that the ACC method strives to maximize the acoustic contrast between the bright zone and the dark zone, but the PM method in the bright zone does not take into account the acoustic contrast between the bright zone and the dark zone. The acoustic contrasts produced by the two proposed methods are mainly between those generated by the ACC method and the PM method in the bright zone. The first proposed method has acoustic contrast greater than 0 dB at most frequencies in 100–1000 Hz for $\mu = 0.1$, $\mu = 0.5$ and $\mu = 0.9$. Only when the frequency is 100 Hz is the acoustic contrast less than 0 dB. The second proposed method has acoustic contrast greater than 0 dB at all frequencies in the range 100–1000 Hz. When using the proposed two methods, the larger the value of μ or τ, the greater the value of acoustic contrast because the larger the value of μ and τ are, the smaller the solution of Equations (25) and (29) will make the square of the sound pressure and radial particle velocity in the dark zone.

The average acoustic contrasts relative to frequency obtained by the different methods are shown in Table 3. The results in Table 3 are basically consistent with those in Figure 4. Additionally, when the weight factor μ and τ take the same value, the average acoustic contrasts obtained by the second proposed method are greater than those obtained by the first proposed method, which indicates that the acoustic contrast performance of the second proposed method is better than that of the first proposed method. The reason is that the second proposed method regulates the reconstruction error of sound pressure and particle velocity in the bright zone, the square of sound pressure and particle velocity in the dark zone, and the square of sound pressure in the dark zone is related to the potential sound energy in the dark zone.

Table 2. The location of related points for experiment 2.

Point	Polar Radius	Azimuthal Angle	Elevation Angle
Center of dark zone	0.6 m	180°	0°
Center of bright zone	0.6 m	0°	0°
Loudspeaker 1	2 m	0°	90°
Loudspeaker 2	2 m	0°	45°
Loudspeaker 3	2 m	45°	45°
Loudspeaker 4	2 m	90°	45°
Loudspeaker 5	2 m	135°	45°
Loudspeaker 6	2 m	180°	45°
Loudspeaker 7	2 m	225°	45°
Loudspeaker 8	2 m	270°	45°
Loudspeaker 9	2 m	315°	45°
Loudspeaker 10	2 m	0°	0°
Loudspeaker 11	2 m	30°	0°
Loudspeaker 12	2 m	60°	0°
Loudspeaker 13	2 m	90°	0°
Loudspeaker 14	2 m	120°	0°
Loudspeaker 15	2 m	150°	0°
Loudspeaker 16	2 m	180°	0°
Loudspeaker 17	2 m	225°	0°
Loudspeaker 18	2 m	270°	0°
Loudspeaker 19	2 m	315°	0°
Loudspeaker 20	2 m	45°	−30°
Loudspeaker 21	2 m	90°	−30°
Loudspeaker 22	2 m	135°	−30°
Origin	0 m	0°	0°
Original source 2	2.5 m	50°	10°

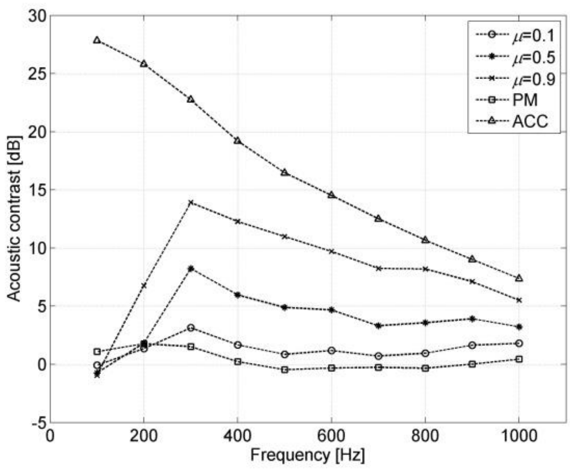

(**a**)

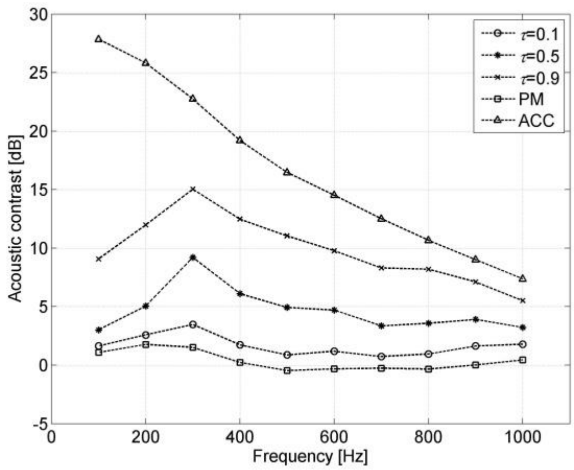

(**b**)

Figure 4. Acoustic contrast of different methods for two-dimensional experiment. (**a**): PM method in bright zone, ACC method, the first proposed method with μ = 0.1, 0.5 and 0.9; (**b**): PM method in bright zone, ACC method, the second proposed method with τ = 0.1, 0.5 and 0.9.

Table 3. Average acoustic contrast of different methods relative to frequency for two-dimensional experiment.

Method	Average Acoustic Contrast (dB)		
PM method in bright zone	0.3708		
ACC method	16.6171		
Proposed method 1	$\mu = 0.1$	$\mu = 0.5$	$\mu = 0.9$
	1.3273	3.8932	8.1772
Proposed method 2	$\tau = 0.1$	$\tau = 0.5$	$\tau = 0.9$
	1.6618	4.7092	9.8529

Figure 5 shows normalized spatial average error comparison of different methods. The ACC method has the highest normalized spatial average error, which can reach up to about 6.6 dB, while the PM method in the bright zone has the lowest normalized spatial average error, and the lowest normalized spatial average error can be close to −60 dB. The reason is that the PM method in the bright zone strives to match the sound pressure between the original and reconstructed sound field in the bright zone, but the ACC method does not consider the sound pressure error between the original and reconstructed sound fields in the bright zone. The normalized spatial average errors generated by the two proposed methods are between those generated by the ACC method and the PM method in the bright zone. The first and the second proposed methods have normalized spatial average error lower than 0 dB at all frequencies in the range 100–1000 Hz for different values of μ and τ. When using the proposed two methods, the smaller the value of μ or τ, the smaller the value of the normalized spatial average error because the smaller the value of μ and τ are, the smaller the solution of Equations (25) and (29) will make the reconstruction error of the sound pressure and radial particle velocity in the bright zone.

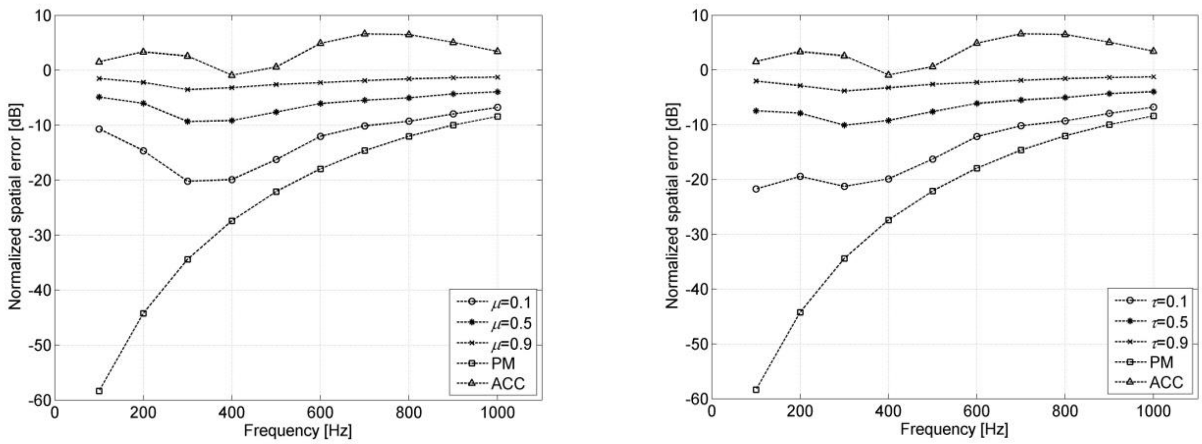

(**a**) (**b**)

Figure 5. Normalized spatial average error of different methods for two-dimensional experiment. (**a**): PM method in bright zone, ACC method, the first proposed method with μ = 0.1, 0.5 and 0.9, respectively; (**b**): PM method in bright zone, ACC method, the second proposed method with τ = 0.1, 0.5 and 0.9, respectively.

Table 4 shows the mean normalized spatial average errors of different methods relative to frequency. The results in Table 4 are basically consistent with those in Figure 5. Additionally, when the weight factor μ and τ take the same value, the mean normalized spatial average errors obtained by the second proposed method are lower than those obtained by the first proposed method, which indicates that the normalized spatial average error performance of the second proposed method is better than that of the first proposed method. The reason is that the second proposed method pays more attention to sound pressure than the first proposed method, and the reconstruction error of the sound pressure in the bright zone is related to the index of reproduction error.

Table 4. Mean normalized spatial average error of different methods relative to frequency for two-dimensional experiment.

Method	Mean Reproduction Error (dB)		
PM method in bright zone	−24.9249		
ACC method	3.3761		
Proposed method 1	$\mu = 0.1$	$\mu = 0.5$	$\mu = 0.9$
	−12.7643	−6.1636	−2.1211
Proposed method 2	$\tau = 0.1$	$\tau = 0.5$	$\tau = 0.9$
	−14.4822	−6.7061	−2.2764

Figure 6 shows the loudspeaker array effort comparison of different methods. The ACC method has the highest loudspeaker array effort, which is close to 0 dB. The loudspeaker array efforts of the PM method in the bright zone are lower than those of the ACC method. The first proposed method has the loudspeaker array effort lower than the ACC method and the PM method in the bright zone at all frequencies in the range 100–1000 Hz. The second proposed method has loudspeaker array effort lower than the ACC method and the PM method in the bright zone at all frequencies in the range 100–1000 Hz except 100 Hz, and τ = 0.5. The study in reference [44] shows that when the loudspeaker array is non-uniformly placed, the control of particle velocity in a single region can obtain more stable loudspeaker strengths than the control of sound pressure in a single region. Both proposed methods pay attention to particle velocity, so they produce lower array efforts than the ACC method and the PM method in the bright zone for most frequencies when loudspeakers are non-uniformly arranged. When using the proposed two methods, the larger the value of μ or τ, the smaller the value of the loudspeaker array effort. The reason may be that the larger the value of μ and τ are, the smaller the solution of Equations (25) and (29) will make the square of the sound pressure and radial particle velocity in the dark zone, which leads to a more stable system.

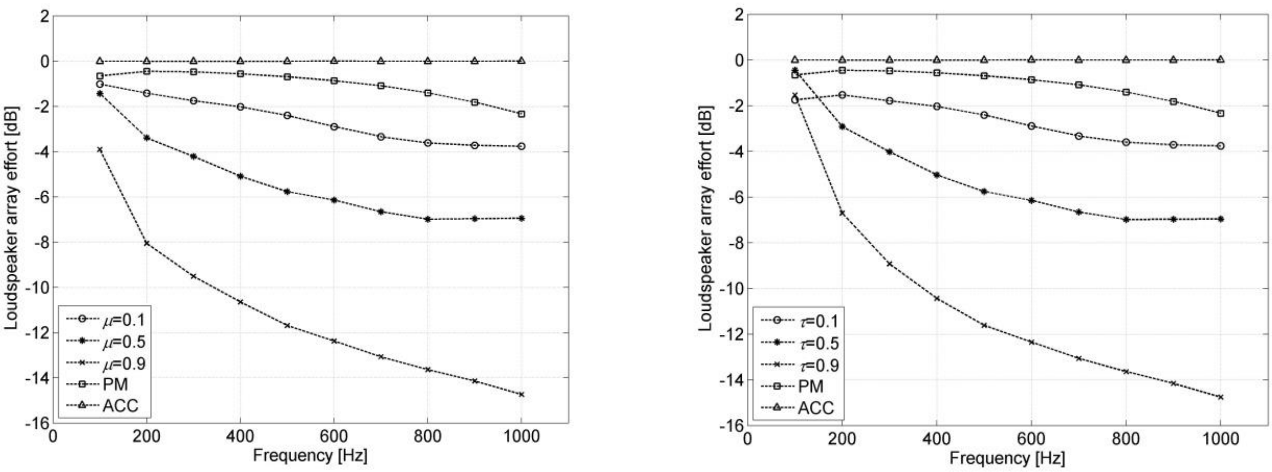

(**a**) (**b**)

Figure 6. Array effort of different methods for two-dimensional experiment. (**a**): PM method in bright zone, ACC method, the first proposed method with μ = 0.1, 0.5 and 0.9; (**b**): PM method in bright zone, ACC method, the second proposed method with τ = 0.1, 0.5 and 0.9.

Table 5 shows the average array effort of different methods relative to frequency. The results in Table 5 are basically consistent with those in Figure 6. When the weight factor

μ and τ take the same value, and the average array efforts obtained by the first proposed method are lower than those obtained by the second proposed method except that the weight factor is 0.1, which indicates that the loudspeaker array effort performance of the first proposed method is better than that of the second proposed method. The reason may be that the first proposed method only focuses on particle velocity, but the second proposed method pays attention to sound pressure as well as particle velocity. The second proposed method focuses on more physical properties, which causes the system to become relatively unstable.

Table 5. Average array effort of different methods relative to frequency for two-dimensional experiment.

Method	Average Array Effort (dB)		
PM method in bright zone	−1.0336		
ACC method	0		
Proposed method 1	$\mu = 0.1$	$\mu = 0.5$	$\mu = 0.9$
	−2.5943	−5.3600	−11.1795
Proposed method 2	$\tau = 0.1$	$\tau = 0.5$	$\tau = 0.9$
	−2.6802	−5.1900	−10.7222

4.3.2. Three-Dimensional Experiment for 22-Channel System

In this part, we have conducted comparative experiments on the 22-channel system similar to Section 4.3.1. On the whole, the variation trend of the experimental indexes produced by different comparison methods is basically consistent with that in Section 4.3.1, and the reasons have been analyzed in Section 4.3.1. Below, we describe the experimental results in detail.

Figure 7 shows acoustic contrast comparison of the different methods for three-dimensional experiment. The ACC method has the highest acoustic contrast, the PM method in the bright zone has the lowest acoustic contrast for most frequencies. For most frequencies, the acoustic contrasts of PM method in the bright zone are less than 0 dB. The first and second proposed methods have acoustic contrast greater than 0 dB at all frequencies in the range 100–1000 Hz. For the proposed two methods, larger values of μ or τ produce greater values of acoustic contrast, which is consistent with the result of the two-dimensional experiment. The average acoustic contrasts relative to frequency obtained by the different methods are shown in Table 6, which are basically consistent with the results in Figure 7.

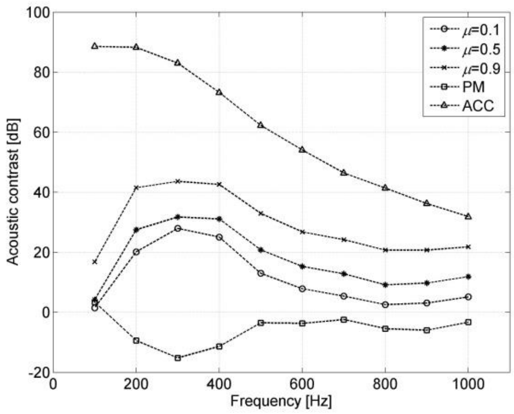

(**a**)

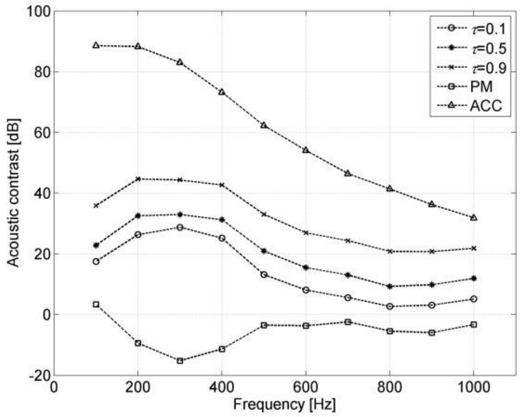

(**b**)

Figure 7. Acoustic contrast of different methods for three-dimensional experiment. (**a**): PM method in bright zone, ACC method, the first proposed method with μ = 0.1, 0.5 and 0.9; (**b**): PM method in bright zone, ACC method, the second proposed method with τ = 0.1, 0.5 and 0.9.

Table 6. Average acoustic contrast of different methods relative to frequency for three-dimensional experiment.

Method	Average Acoustic Contrast (dB)		
PM method in bright zone	−5.6907		
ACC method	60.5338		
Proposed method 1	$\mu = 0.1$	$\mu = 0.5$	$\mu = 0.9$
	11.1659	17.4275	29.1630
Proposed method 2	$\tau = 0.1$	$\tau = 0.5$	$\tau = 0.9$
	13.5441	20.0006	31.5162

Figure 8 shows the normalized spatial average error comparison of the different methods for the three-dimensional experiment. The ACC method has the highest normalized spatial average error, which can reach up to nearly 10 dB, while the PM method in the bright zone has the lowest normalized spatial average error, and the lowest normalized spatial average error can be close to −90 dB. The normalized spatial average errors of the two proposed methods are between the ACC and the PM methods in the bright zone. The normalized spatial average errors of the first proposed method are less than 0 dB. The normalized spatial average errors of the second proposed method are less than −5 dB. The smaller the value of μ or τ, the smaller the value of normalized spatial average error of the two proposed methods. Table 7 shows the mean normalized spatial average error of the different methods relative to frequency. The variation of the mean normalized spatial average error of the different methods is consistent with Figure 8.

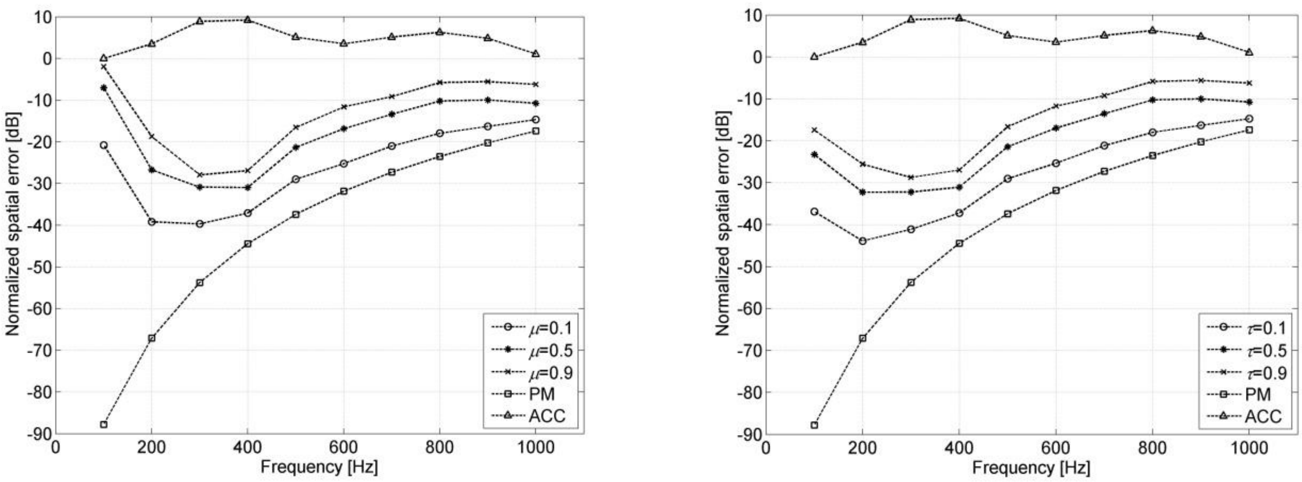

(**a**) (**b**)

Figure 8. Normalized spatial average error of different methods for three-dimensional experiment. (**a**): PM method in bright zone, ACC method, the first proposed method, with μ = 0.1, 0.5 and 0.9, respectively; (**b**): PM method in bright zone, ACC method, the second proposed method, with τ = 0.1, 0.5 and 0.9, respectively.

Figure 9 shows the loudspeaker array effort comparison of the different methods. The PM method in the bright zone has the highest loudspeaker array efforts for most frequencies, which are larger than 0 dB. The loudspeaker array efforts of the ACC method are lower than those of the PM method in the bright zone. The two proposed methods have loudspeaker array efforts lower than the PM method in the bright zone at most frequencies in the range 100–1000 Hz except 100 Hz. The two proposed methods have loudspeaker array efforts lower than the ACC method at most frequencies in the range 100–1000 Hz, except 100 Hz, 200 Hz and 600 Hz.

Table 7. Mean normalized spatial average error of different methods relative to frequency for three-dimensional experiment.

Method	Mean Reproduction Error (dB)		
PM method in bright zone	−41.0681		
ACC method	4.7704		
Proposed method 1	$\mu = 0.1$	$\mu = 0.5$	$\mu = 0.9$
	−26.0711	−17.7933	−13.0315
Proposed method 2	$\tau = 0.1$	$\tau = 0.5$	$\tau = 0.9$
	−28.3474	−20.1580	−15.3868

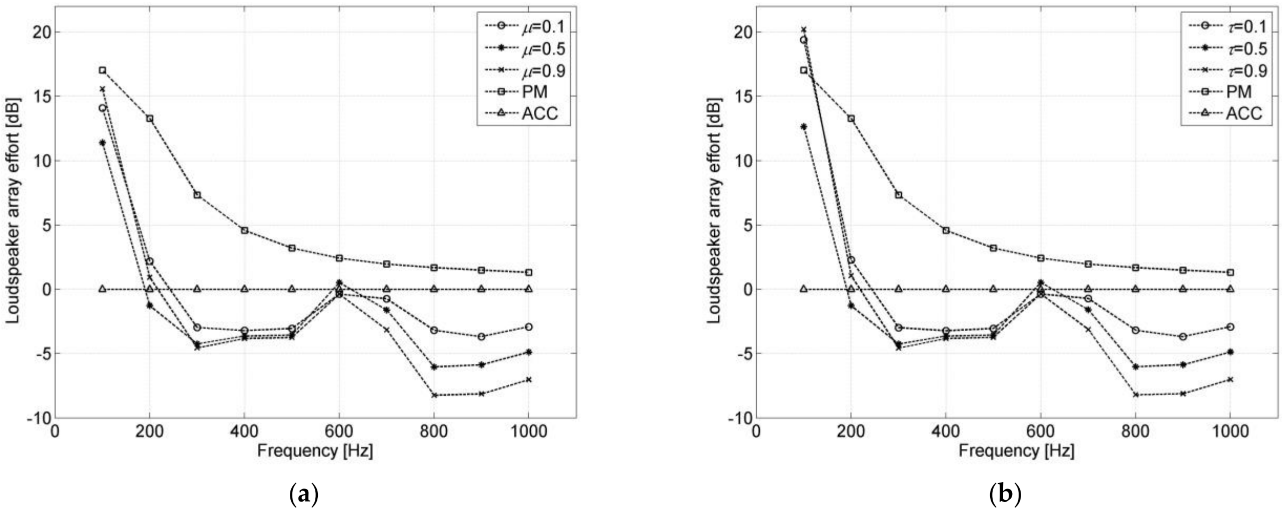

Figure 9. Array effort of different methods for three-dimensional experiment. (**a**): PM method in bright zone, ACC method, the first proposed method, with μ = 0.1, 0.5 and 0.9, respectively; (**b**): PM method in bright zone, ACC method, the second proposed method, with τ = 0.1, 0.5 and 0.9, respectively.

Table 8 shows the average array efforts of the different methods relative to frequency. From it we can see that the PM method in the bright zone has the highest average array effort. The average array effort of the ACC method is about 0 dB and is higher than those of the first proposed method for all weight factor values. Additionally the average array effort of the ACC method is higher than those of the second proposed method for τ = 0.5 and τ = 0.9.

Table 8. Average array effort of different methods relative to frequency for three-dimensional experiment.

Method	Average Array Effort (dB)		
PM method in bright zone	5.4324		
ACC method	0		
Proposed method 1	$\mu = 0.1$	$\mu = 0.5$	$\mu = 0.9$
	−0.3828	−1.9186	−2.2565
Proposed method 2	$\tau = 0.1$	$\tau = 0.5$	$\tau = 0.9$
	0.1577	−1.7869	−1.7695

From Tables 3 and 6, we can see that the average acoustic contrasts of the ACC method and the two proposed methods in the three-dimensional experiment are much higher than those of the ACC method and the two proposed methods in the two-dimensional experiment, respectively. However, the average acoustic contrast of the PM method in the bright zone in the three-dimensional experiment is lower than that of the PM method in the bright zone in the two-dimensional experiment. From Tables 4 and 7, we can see that the mean normalized spatial average errors of the PM method in the bright zone and the two proposed methods in three-dimensional experiment are much lower than those of the PM method in the bright zone and the two proposed methods in two-dimensional experiment, respectively. However, the mean normalized spatial average error of the ACC method in the three-dimensional experiment is higher than that of the ACC method in the two-dimensional experiment. The reason may be that the radius of the bright zone and the dark zone in the two-dimensional and three-dimensional experiments are the same, but in three-dimensional experiment there are 22 loudspeakers, much more than the 5 loudspeakers in the two-dimensional experiment. From Tables 5 and 8, we can see that the average array efforts of the PM method in the bright zone and the two proposed methods in the three-dimensional experiment are higher than those of the PM method in the bright zone and the two proposed methods in the two-dimensional experiment, respectively. The average array effort of the ACC method in the three-dimensional experiment is equal to that of the ACC method in the two-dimensional experiment. The reason may be that in the two-dimensional experiment, the original sound source is located in the same horizontal plane as the five loudspeakers; in the three-dimensional experiment, though, there are more loudspeakers used, and the original sound source is off the horizontal plane and in a position where loudspeakers are relatively rare. When the loudspeakers are non-uniformly placed or there are few loudspeakers around the original sound source, the PM method in the bright zone is not stable.

4.3.3. Influence of Sampling Point Spacing on Reconstruction Effect

For this part, we set the interval of sampling points to 0.08 m, which is more than twice the interval of the sampling points in Sections 4.3.1 and 4.3.2. The rest of the settings are the same as Sections 4.3.1 and 4.3.2. The sampling points in this part are called sparse sampling points. The average acoustic contrast, mean normalized spatial average error and average array effort of the different methods relative to frequency with 5-channel and 22-channel systems are shown in Tables 9–14.

Table 9. Average acoustic contrast of different methods relative to frequency for two-dimensional experiment with sparse sampling points.

Method	Average Acoustic Contrast (dB)		
PM method in bright zone	0.2994		
ACC method	19.4578		
Proposed method 1	$\mu = 0.1$	$\mu = 0.5$	$\mu = 0.9$
	1.6066	4.7592	9.7326
Proposed method 2	$\tau = 0.1$	$\tau = 0.5$	$\tau = 0.9$
	1.9790	5.5702	11.4291

Table 10. Mean normalized spatial average error of different methods relative to frequency for two-dimensional experiment with sparse sampling points.

Method	Mean Reproduction Error (dB)		
PM method in bright zone	−26.9763		
ACC method	3.3539		
Proposed method 1	$\mu = 0.1$	$\mu = 0.5$	$\mu = 0.9$
	−13.2347	−6.4501	−2.3426
Proposed method 2	$\tau = 0.1$	$\tau = 0.5$	$\tau = 0.9$
	−14.9982	−6.9689	−2.5227

Table 11. Average array effort of different methods relative to frequency for two-dimensional experiment with sparse sampling points.

Method	Average Array Effort (dB)		
PM method in bright zone	−0.9110		
ACC method	0		
Proposed method 1	$\mu = 0.1$	$\mu = 0.5$	$\mu = 0.9$
	−2.6142	−5.2061	−10.2084
Proposed method 2	$\tau = 0.1$	$\tau = 0.5$	$\tau = 0.9$
	−2.7225	−5.0080	−9.7409

Table 12. Average acoustic contrast of different methods relative to frequency for three-dimensional experiment with sparse sampling points.

Method	Average Acoustic Contrast (dB)		
PM method in bright zone	−5.8793		
ACC method	64.7319		
Proposed method 1	$\mu = 0.1$	$\mu = 0.5$	$\mu = 0.9$
	11.9858	18.1954	29.7968
Proposed method 2	$\tau = 0.1$	$\tau = 0.5$	$\tau = 0.9$
	14.5908	20.9809	32.4661

Table 13. Mean normalized spatial average error of different methods relative to frequency for three-dimensional experiment with sparse sampling points.

Method	Mean Reproduction Error (dB)		
PM method in bright zone	−44.7588		
ACC method	4.5444		
Proposed method 1	$\mu = 0.1$	$\mu = 0.5$	$\mu = 0.9$
	−27.2686	−18.6784	−13.8401
Proposed method 2	$\tau = 0.1$	$\tau = 0.5$	$\tau = 0.9$
	−29.6759	−21.2740	−16.4592

Table 14. Average array effort of different methods relative to frequency for three-dimensional experiment with sparse sampling points.

Method	Average Array Effort (dB)		
PM method in bright zone	6.5094		
ACC method	0		
Proposed method 1	$\mu = 0.1$	$\mu = 0.5$	$\mu = 0.9$
	−0.1474	−1.5661	−1.8415
Proposed method 2	$\tau = 0.1$	$\tau = 0.5$	$\tau = 0.9$
	0.2578	−1.4842	−1.4802

Compared with Tables 3–8, when the sampling point density becomes sparse, the average acoustic contrasts of the different methods increase except for the PM method in the bright zone, and the mean normalized spatial average errors of the different methods decrease, but the average array efforts of the different methods increase except for the

ACC method and the proposed two methods with weight factor being 0.1 for the two-dimensional experiment. The reason may be that the acoustic contrast and normalized spatial average error involve averaging and the fewer sample points, the better the calculation performance. The PM method in the bright zone requires the matrix inverse and is limited by the matrix condition number. In the case of sparse sampling points, the systems become relatively unstable due to the small number of sampling points.

4.3.4. Discussion

Except for a few frequencies, the results of the two-dimensional and three-dimensional experiments are generally similar. There is a trade-off between three indicators: acoustic contrast, reproduction error and array effort [31,34,47]. If one of these three indicators is better, the other indicators are likely to be worse. The PM method in the bright zone is mainly concerned with matching the sound pressure between the original and reconstructed sound fields in the bright zone, so it has minimal reproduction error but performs poorly in the acoustic contrast and array efforts. The ACC method focuses on maximizing the acoustic contrast between the bright zone and the dark zone, so it has the highest acoustic contrast, but it underperforms on reproduction error and array effort. Both the PM method in the bright zone and the ACC method only focus on a certain index, which is a relatively extreme method. Therefore, they perform exceptionally well in one index and poorly in the rest. The first proposed method regulates the reconstruction error of the radial particle velocity in the bright zone and the square of radial particle velocity in the dark zone. The second proposed method regulates the reconstruction error of the sound pressure and radial particle velocity in the bright zone and the sound energy and square of radial particle velocity in the dark zone. The proposed two methods comprehensively consider the physical property of sound in both the bright zone and the dark zone. As a whole, the acoustic contrasts and reproduction errors generated by the two proposed methods are between those generated by the ACC method and the PM method in the bright zone, but the array efforts of the two proposed methods are lower than those of the ACC method and the PM method in the bright zone.

5. Conclusions

The traditional methods mainly use sound pressure recovery in the bright zone to control the sound field. When the loudspeakers are sparsely placed, the reconstruction system is easily unstable. To solve this problem, two sound field control methods are proposed in this paper: one is based on particle velocity, and the other is based on sound pressure and particle velocity. For the convenience of problem processing, radial particle velocity is actually used. In the first proposed method, the weight factor μ is introduced to adjust the reconstruction error of the radial particle velocity in the bright zone and the square of radial particle velocity in the dark zone. The second proposed method builds the model in a similar way but considers both the sound pressure and radial particle velocity in the bright zone and the dark zone. By changing the value of the weight factor in the range of 0 to 1, the performance of the two proposed methods can be changed. Simulation experiments compared the performance of the traditional and proposed methods in terms of acoustic contrast, reproduction error, array effort and their means relative to frequency. The experimental results show that the ACC method has the largest acoustic contrast and reproduction error; the PM method in the bright zone has the minimum acoustic contrast for most frequencies and the minimum reproduction error; the array efforts of the ACC and PM methods in the bright zone are higher than those of the proposed methods for most frequencies. The proposed two methods achieve a good compromise in aspects of acoustic contrast, reproduction error and array effort. Their array effort values are lower than these traditional methods for most frequencies, so they can ensure the robustness of the reconstruction system better. For the two-dimensional case, the maximum reduction of the average array effort generated by the proposed methods is about 10 dB compared with the average array effort generated by the PM method in the bright zone, and about

11 dB compared with the average array effort generated by the ACC method. For the three-dimensional case, the maximum reduction of the average array effort generated by the proposed methods is about 8 dB compared with the average array effort generated by the PM method in the bright zone, and about 2 dB compared with the average array effort generated by the ACC method. Among the two proposed methods, the second method has higher average acoustic contrasts, lower mean reproduction errors, and its average array efforts are slightly greater than the first method for most weight factors. For two-dimensional and three dimensional cases, the maximum increase of the average array effort generated by the second proposed method is about 0.5 dB compared with that generated by the first proposed method. Therefore, the second method is a better alternative sound field control method.

Author Contributions: Conceptualization, S.W. and C.Z.; Formal analysis, S.W.; Funding acquisition, S.W. and C.Z.; Investigation, S.W.; Method-ology, S.W.; Supervision, C.Z.; Validation, S.W.; Writing—original draft, S.W.; Writing—review & editing, S.W. and C.Z. All authors have read and agreed to the published version of the manuscript.

Funding: This work was supported in part by Wuhan Polytechnic University Scientific Research Project (No. 2019RZ02), Hubei Provincial Major Science and Technology Special Projects (No. 2018ABA099).

Conflicts of Interest: The authors declare no conflict of interest.

References

1. Fellgett, P.B. Ambisonic reproduction of directionality in surround sound systems. *Nature* **1974**, *252*, 534–538. [CrossRef]
2. Gerzon, M.A. Ambisonics in multichannel broadcasting and video. *J. Audio Eng. Soc.* **1985**, *33*, 859–871.
3. Kirkeby, O.; Nelson, P.A. Reproduction of plane wave sound fields. *J. Acoust. Soc. Am.* **1993**, *94*, 2992–3000. [CrossRef]
4. Berkhout, A.J.; de Vries, D.; Vogel, P. Acoustic control by wave field synthesis. *J. Acoust. Soc. Am.* **1993**, *93*, 2764–2778. [CrossRef]
5. Ise, S. A principle of sound field control based on the Kirchhoff-Helmholtz integral equation and the theory of inverse systems. *Acta Acust. Acust.* **1999**, *85*, 78–87.
6. Ward, D.B.; Abhayapala, T.D. Reproduction of a plane-wave sound field using an array of loudspeakers. *IEEE Trans. Speech Audio Proc.* **2001**, *9*, 697–707. [CrossRef]
7. Daniel, J.; Nicol, R.; Moreau, S. Further investigations of high order ambisonics and wave field synthesis for holophonic sound imaging. In Proceedings of the 114th Audio Engineering Society Convention, Amsterdam, The Netherlands, 22–25 March 2003; p. 5788.
8. Poletti, M.A. Three-dimensional surround sound systems based on spherical harmonics. *J. Audio Eng. Soc.* **2005**, *53*, 1004–1025.
9. Wu, Y.J.; Abhayapala, T.D. Theory and design of sound field reproduction using continuous loudspeaker concept. *IEEE Trans. Audio Speech Lang. Proc.* **2009**, *17*, 107–116. [CrossRef]
10. Wu, Y.J.; Abhayapala, T.D. Spatial multizone soundfield reproduction: Theory and design. *IEEE Trans. Audio Speech Lang. Proc.* **2011**, *19*, 1711–1720. [CrossRef]
11. Poletti, M.A.; Betlehem, T.; Abhayapala, T.D. Analysis of 2D sound reproduction with fixed-directivity loudspeakers. In Proceedings of the 2012 IEEE International Conference on Acoustics, Speech and Signal Processing (ICASSP), Kyoto, Japan, 25–30 March 2012; pp. 377–380.
12. Zhang, W.; Abhayapala, T.D. 2.5D sound field reproduction in higher order Ambisonics. In Proceedings of the 14th International Workshop on Acoustic Signal Enhancement (IWAENC), Juan-les-Pins, France, 8–11 September 2014; pp. 342–346.
13. Zhou, L.; Jia, M.; Bao, C.; Bu, B. Multi-source sound field reproduction using cylindrical harmonic analysis. In Proceedings of the 2014 IEEE China Summit & International Conference on Signal and Information Processing (ChinaSIP), Xi'an, China, 9–13 July 2014; pp. 129–132.
14. Zhang, W.; Abhayapala, T.D. Three dimensional sound field reproduction using multiple circular loudspeaker arrays: Functional analysis guided approach. *IEEE ACM Trans. Audio Speech Lang. Proc.* **2014**, *22*, 1184–1194. [CrossRef]
15. Winter, F.; Spors, S. Physical properties of local wave field synthesis using circular loudspeaker arrays. In Proceedings of the 10th European Congress and Exposition on Noise Control Engineering, Maastricht, The Netherlands, 1–3 June 2015; pp. 263–268.
16. Firtha, G.; Fiala, P.; Schultz, F.; Spors, S. Improved referencing schemes for 2.5D wave field synthesis driving functions. *IEEE ACM Trans. Audio Speech Lang. Proc.* **2017**, *25*, 1117–1127. [CrossRef]
17. Wierstorf, H.; Hold, C.; Raake, A. Listener preference for wave field synthesis, stereophony, and different mixes in popular music. *J. Audio Eng. Soc.* **2018**, *66*, 385–396.
18. Firtha, G.; Fiala, P.; Schultz, F.; Spors, S. On the general relation of wave field synthesis and spectral division method for linear arrays. *IEEE ACM Trans. Audio Speech Lang. Proc.* **2018**, *26*, 2393–2403. [CrossRef]
19. Otani, M.; Shigetani, H. Reproduction accuracy of higher-order ambisonics with max-re and/or least norm solution in decoding. *Acoust. Sci. Technol.* **2019**, *40*, 23–28. [CrossRef]

20. Ueno, N.; Koyama, S.; Saruwatari, H. Three-dimensional sound field reproduction based on weighted mode-matching method. *IEEE ACM Trans. Audio Speech Lang. Proc.* **2019**, *27*, 1852–1867. [CrossRef]
21. Winter, F.; Schultz, F.; Firtha, G.; Spors, S. A geometric model for prediction of spatial aliasing in 2.5D sound field synthesis. *IEEE ACM Trans. Audio Speech Lang. Proc.* **2019**, *27*, 1031–1046. [CrossRef]
22. Choi, J.-W.; Kim, Y.-H. Generation of an acoustically bright zone with an illuminated region using multiple sources. *J. Acoust. Soc. Am.* **2002**, *111*, 1695–1700. [CrossRef]
23. Elliott, S.J.; Jones, M. An active headrest for personal audio. *J. Acoust. Soc. Am.* **2006**, *119*, 2702–2709. [CrossRef]
24. Jones, M.; Elliott, S.J. Personal audio with multiple dark zones. *J. Acoust. Soc. Am.* **2008**, *124*, 3497–3506. [CrossRef]
25. Chang, J.-H.; Lee, C.-H.; Park, J.-Y.; Kim, Y.-H. A realization of sound focused personal audio system using acoustic contrast control. *J. Acoust. Soc. Am.* **2009**, *125*, 2091–2097. [CrossRef]
26. Shin, M.-C.; Lee, S.-Q.; Fazi, F.M.; Nelson, P.A.; Kim, D.-S.; Wang, S.-M.; Park, K.-H.; Seo, J.-I. Maximization of acoustic energy difference between two spaces. *J. Acoust. Soc. Am.* **2010**, *128*, 121–131. [CrossRef] [PubMed]
27. Kim, D.; Kim, K.; Wang, S.; Lee, S.; Crocker, M.J. Maximization of the directivity ratio with the desired audible gain level for broadband design of near field loudspeaker arrays. *J. Sound Vib.* **2011**, *330*, 5517–5529. [CrossRef]
28. Møller, M.; Olsen, M.; Jacobsen, F. A hybrid method combining synthesis of a sound field and control of acoustic contrast. In Proceedings of the 132nd AES Convention, Budapest, Hungary, 26–29 April 2012; p. 8627.
29. Chang, J.-H.; Jacobsen, F. Sound field control with a circular double-layer array of loudspeakers. *J. Acoust. Soc. Am.* **2012**, *131*, 4518–4525. [CrossRef] [PubMed]
30. Poletti, M. An investigation of 2D multizone surround sound systems. In Proceedings of the 125th AES Convention, San Francisco, CA, USA, 2–5 October 2008; p. 7551.
31. Bai, M.R.; Wen, J.-C.; Hsu, H.; Hua, Y.-H.; Hsieh, Y.-H. Investigation on the reproduction performance versus acoustic contrast control in sound field synthesis. *J. Acoust. Soc. Am.* **2014**, *136*, 1591–1600. [CrossRef] [PubMed]
32. Olivieri, F.; Fazi, F.M.; Shin, M.; Nelson, P.A. Pressure-Matching beamforming method for loudspeaker arrays with frequency dependent selection of control points. In Proceedings of the 138th AES Convention, Warsaw, Poland, 7–10 May 2015; p. 9322.
33. Olivieri, F.; Fazi, F.M.; Nelson, P.A.; Fontana, S. Comparison of strategies for accurate reproduction of a target signal with compact arrays of loudspeakers for the generation of zones of private sound and silence. *J. Audio Eng. Soc.* **2016**, *64*, 905–917. [CrossRef]
34. Olivieri, F.; Fazi, F.M.; Fontana, S.; Menzies, D.; Nelson, P.A. Generation of private sound with a circular loudspeaker array and the weighted pressure matching method. *IEEE ACM Trans. Audio Speech Lang. Proc.* **2017**, *25*, 1579–1591. [CrossRef]
35. Badajoz, J.; Chang, J.-H.; Agerkvist, F.T. Reproduction of nearby sources by imposing true interaural differences on a sound field control approach. *J. Acoust. Soc. Am.* **2015**, *138*, 2387–2398. [CrossRef]
36. Afghah, T.; Patros, E.; Puckette, M. A pseudoinverse technique for the pressure-matching beamforming method. In Proceedings of the 145th AES Convention, New York, NY, USA, 17–20 October 2018; p. 10052.
37. Liao, X.; Zheng, S.; Wang, Y.; Peng, B. A control method for balancing the reproductive performance and the acoustic contrast performance in a personal audio system. *Acta Acust.* **2018**, *43*, 835–842.
38. Lee, T.; Nielsen, J.K.; Christensen, M.G. Towards perceptually optimized sound Zones: A proof-of-concept study. In Proceedings of the 2019 IEEE International Conference on Acoustics, Speech and Signal Processing (ICASSP), Brighton, UK, 12–17 May 2019; pp. 136–140.
39. Lee, T.; Nielsen, J.K.; Christensen, M.G. Signal-adaptive and perceptually optimized sound zones with variable span trade-off filters. *IEEE ACM Trans. Audio Speech Lang. Proc.* **2020**, *28*, 2412–2426. [CrossRef]
40. Lee, T.; Shi, L.; Nielsen, J.K.; Christensen, M.G. Fast generation of sound zones using variable span trade-off filters in the DFT-domain. *IEEE ACM Trans. Audio Speech Lang. Proc.* **2021**, *29*, 363–378. [CrossRef]
41. Shin, M.; Fazi, F.M.; Nelson, P.A.; Hirono, F.C. Controlled sound field with a dual layer loudspeaker array. *J. Sound Vib.* **2014**, *333*, 3794–3817. [CrossRef]
42. Ryu, H.; Wang, S.; Kim, S.M. Development of a personal audio performance controller with efficient, fine, and linear tunable functions. *IEEE Access* **2020**, *8*, 123916–123928. [CrossRef]
43. Choi, J.-W. Real-time demonstration of personal audio and 3d audio rendering using line array systems. In Proceedings of the International Conference on MultiMedia Modeling, Daejeon, Korea, 5–8 January 2020; pp. 734–738.
44. Shin, M.; Nelson, P.A.; Fazi, F.M.; Seo, J. Velocity controlled sound field reproduction by non-uniformly spaced loudspeakers. *J. Sound Vib.* **2016**, *370*, 444–464. [CrossRef]
45. Pierce, A.D. *Acoustics, an Introduction to Its Physical Principles and Applications*; Acoustical Society of America: New York, NY, USA, 1989.
46. Sawaya, I.; Oode, S.; Ando, A.; Hamasaki, K. Size and shape of listening area reproduced by three-dimensional multichannel sound system with various numbers of loudspeakers. In Proceedings of the 131th AES Convention, New York, NY, USA, 20–23 October 2011; p. 8510.
47. Coleman, P.; Jackson, P.J.B.; Olik, M.; Møller, M.; Olsen, M.; Pedersen, J.A. Acoustic contrast, planarity and robustness of sound zone methods using a circular loudspeaker array. *J. Acoust. Soc. Am.* **2014**, *135*, 1929–1940. [CrossRef] [PubMed]